All-Fiber Optical Magnetic Field Sensor Based on Faraday Rotation in Highly Terbium Doped Fiber

Magnetic field sensors have been widely used for navigation, vehicle detection, current sensing, and spatial and geophysical research. Many techniques developed for magnetic field sensors are based on electronics, including superconducting quantum interference devices (SQUID's), search coils, fluxgates, Hall-effect sensors, anisotropic magnetoresistive devices, and giant magnetoresistive devices.[1] All-fiber optical magnetic field sensors are desirable because of their immunity to electromagnetic interference, low weight, small size, and long-distance signal transmission for remote operation.

Many all-fiber magnetic field sensors use material coatings. For example, if a magnetostrictive or metal jacket is deposited on the fiber, the optical phase can be changed by strain or Lorentzian force, respectively, when immersed in a magnetic field.[2,3] In another method, a fiber end is coated with a composite material and butt coupled to another fiber. The optical coupling between the fibers changes with the transverse displacement of the coated fiber in the magnetic field.[4] In yet another method, iron film is deposited on a side-polished fiber Bragg grating. The reflective wavelength of the fiber grating shifts with the strain induced by a magnetic field.[5]

Faraday rotation can also be used for magnet sensors. Because the Verdet constant of silica fiber is small [~1.1 rad/(Tm) at 1064 nm], the fiber is usually coiled multiturn to increase the polarization rotation angle. This kind of magnet sensor is often used for current sensing.[6,7] However, bend-induced linear birefringence affects the state of polarization and quenches the desired Faraday effect. In this article, an all-fiber optical magnet sensor based on Faraday rotation is demonstrated. The device is made of a fiber Faraday rotator spliced to a fiber polarizer. The fiber Faraday rotator is a 2-cm-long terbium-doped (Tb) fiber, which is sufficiently short to avoid bending. The fiber polarizer is Corning SP1060 single-polarization fiber (PZ).

The magnetic sensing principle is shown in Fig. 120.44. Linear-polarized input light from the laser source is transmitted to the Tb fiber via polarization-maintaining (PM) fiber. The polarization of the light rotates when the Tb fiber experiences a magnetic field along the axis of light propagation. The light then goes through the fiber polarizer, which extinguishes light whose polarization is not aligned to its principle axis. PM fiber transmits the remaining light to a detector. Because of the polarizer, the power received at the detector is a function of the polarization rotation angle given by Malus' Law.[8] Since the polarization rotation angle in the Tb fiber is related to the magnetic field strength by the Faraday effect, the magnetic field can be measured by monitoring the output power of the sensor.

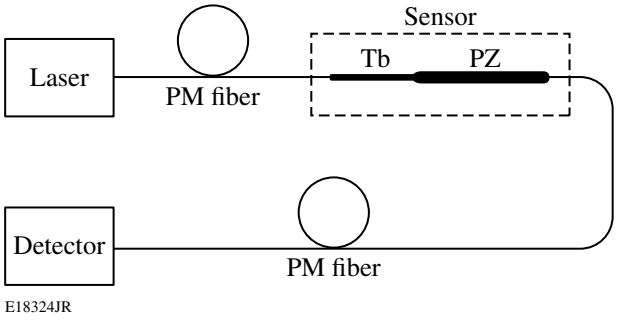

Figure 120.44
Sensing principle of an all-fiber Faraday magnet sensor. PZ: single-polarization fiber; PM: polarization-maintaining fiber.

Terbium doping is an effective way to increase the Verdet constant in the fiber to reduce the fiber length and avoid coiling. Highly terbium doped silicate glasses were designed and fabricated. Boron oxide and aluminum oxide were added into the glass composition to improve the solubility of terbium oxide. Fifty-six-wt% terbium-oxide–doped glass is used as the core glass. The rod-in-tube technique was used for single-mode fiber fabrication. The fiber pulling temperature is around 1000°C. The N.A. and diameter of the core are 0.14 and 4 μm, and cladding diameter of the fiber is 130 μm. The propagation loss of the fiber is measured to be 0.11 dB/cm at 1310 nm using the cutback technique. The effective Verdet constant was measured to be -24.5 ± 1.0 rad/(Tm), using the measurement technique described in Refs. 9 and 10.

Single-polarization fiber is a type of fiber in which only one polarization mode can propagate. This kind of fiber has large birefringence to separate the two orthogonal polarization modes so that each has a different cutoff wavelength. Therefore, within a certain wavelength region, one polarization mode propagates while the other is eliminated because of high loss. In this way, the fiber functions as a polarizer. Such large birefringence can be introduced via stress from boron-doped rods, elliptical core/cladding, or air holes.

In this experiment, Corning SP1060 fiber was used as the polarizing element.[11] With two air holes on either side of an elliptical core, large birefringence and therefore spectrally separated fundamental-mode cutoff were achieved. The core diameter along the major axis was 8 μm, and the clad diameter was 125 μm, with a core N.A. of 0.14. The propagation loss of the surviving mode was 0.1 dB/m at 1060 nm. The center wavelength was 1065 nm and the bandwidth was 25 nm. The polarization extinction ratio was dependent on the length of the fiber. A 1-m PZ fiber was used in the experiment and was coiled with a 15-cm diameter to shift the PZ bandwidth toward the shorter wavelength, resulting in an extinction ratio >16 dB at a 1053-nm working wavelength.

The experimental configuration used to test the sensor is shown in Fig. 120.45. A 2-cm section of Tb-doped fiber, spliced between the PM fiber and 1-m section of PZ fiber, went through a magnet tube. Linearly polarized 1053-nm light was launched into the PM fiber. The polarization directions of the PM and PZ fibers were aligned with a rotational difference of θ_0, which should have been set between 20° to 70° to obtain a nearly linear response curve of magnetic field strength as a function of measured power. The N48 NdFeB magnet tube was 4 cm long with inner and outer diameters of 5 mm and 6 cm, respectively. As the magnet was translated along the fiber, the magnetic field imposed on the Tb fiber changed.

Magnetic fields can be readily calculated by using the geometrical shape of the magnet.[12] The axial component of the magnetic field distribution along the central axis of the magnet tube was derived to be

$$B_z(z) = \frac{B_r}{2}\left\{\frac{z + l/2}{\left[a_1^2 + (z + l/2)^2\right]^{1/2}} - \frac{z + l/2}{\left[a_2^2 + (z + l/2)^2\right]^{1/2}} - \frac{z - l/2}{\left[a_1^2 + (z - l/2)^2\right]^{1/2}} + \frac{z - l/2}{\left[a_2^2 + (z - l/2)^2\right]^{1/2}}\right\}, \quad (1)$$

where a_1 and a_2 are the inner and outer radii, respectively, l is the length of the magnet, and B_r is the residual magnetic flux density. Figure 120.46 shows the calculated $B_z(z)$ for the N48 magnet used in the experiment (B_r = 1.35 T) along with the measured magnetic field outside the magnet. The physical ends of the magnet are also shown for reference. The magnetic field, measured only outside the magnet because the probe size is larger than a_1, agreed very well with the theoretical curve calculated from Eq. (1). The averaged magnetic density flux B_{av} experienced by the 2-cm length of Tb fiber (calculated in the center of Tb fiber) is also shown in the figure. This curve is nearly linear from −3 to −1 cm along the z axis. This region will be used in the measurement.

After considering the extinction ratio of the polarizing fiber, Ex, the relative transmission through the PZ fiber is derived as[13]

$$I/I_0 = \cos^2(\theta_0 + \theta) + \sin^2(\theta_0 + \theta)\,10^{(-\mathrm{Ex}/10)}, \quad (2)$$

where I/I_0 is the measured output power normalized to its maximum I_0, $\theta = VB_{av}L$ is the Faraday rotation angle in the Tb fiber, and V and L are the effective Verdet constant and the length of the Tb fiber, respectively. In the experiment, Ex = 18 dB and $\theta_0 = 50°$. The experimental and theoretical curves of the relative transmission are shown in Fig. 120.47. The error is determined to be 0.01 by a polarization-stability measurement. The experimental data agree well with the theoretical curve, both of which show a nearly linear response. The nominal

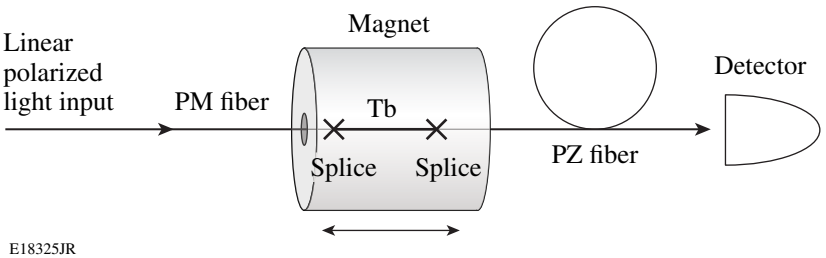

Figure 120.45
Experimental configuration of an all-fiber magnet sensor.

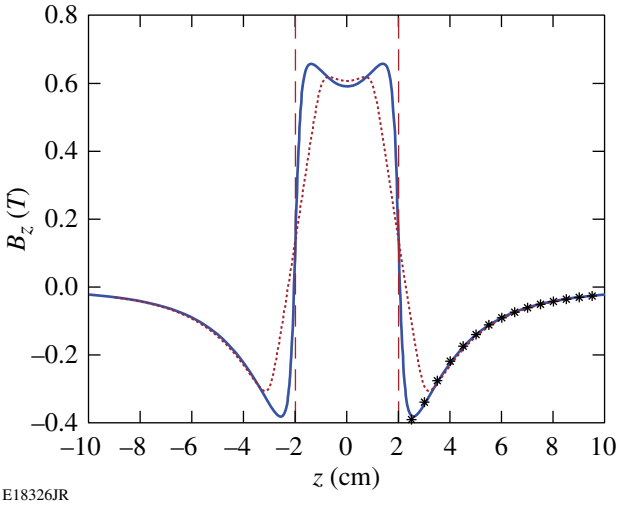

Figure 120.46
Theoretical (solid) and measured (star) magnetic density flux distribution B_z along the center axis z. The dashed lines represent the magnet ends and the dotted line represents B_{av}, the magnetic density flux averaged over a 2-cm length along the axis z.

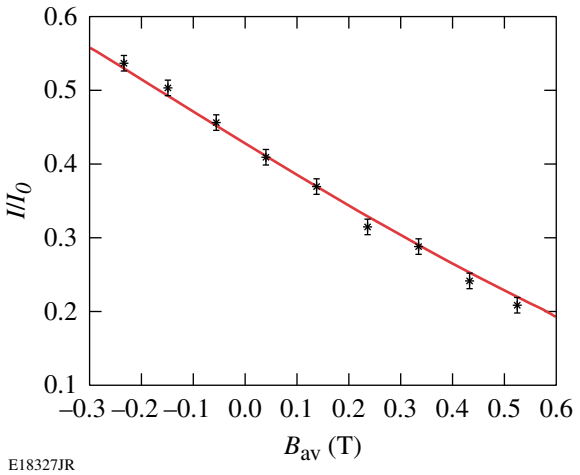

Figure 120.47
Measured (star) and calculated (solid) relative transmission of an all-fiber magnet sensor.

transmission loss through the device is 10 dB, mainly induced by the mode mismatch between the PZ and Tb fibers and the splicing loss between the Tb and silica fibers.

The sensitivity of the all-fiber sensor is given by $d\theta/dB_{av} = VL = 0.49$ rad/T. This can be increased by increasing the effective Verdet constant and/or length of the Tb fiber. Since the polarization rotation may go beyond 90°, a maximum detected magnetic field $B_{max} = (\pi/2)/VL$ of 3.2 T can be measured in this configuration without ambiguity. A larger magnetic field could be measured by decreasing the effective Verdet constant or the length of the Tb fiber.

The resolution of the magnetic sensor is obtained by taking the derivative and absolute value of both sides of Eq. (2):

$$\Delta B = \frac{\Delta I}{I_0 VL \sin\left[2\left(\theta_0 + \theta\right)\right]} = \frac{\Delta I}{I_0} \frac{2B_{max}}{\pi \sin\left[2\left(\theta_0 + \theta\right)\right]}. \quad (3)$$

In this equation, the effect of the extinction ratio was neglected, which is appropriate for Ex > 20. Increasing the effective Verdet constant and the length of the Tb fiber could also help to increase the resolution, at the expense of reducing B_{max}. The most effective way is to decrease the ratio $\Delta I/I_0$. For example, if the detector resolution is at the nW level, increasing I_0 to the mW level yields a sensor resolution of 2.0×10^{-6} T, with B_{max} still at 3.2 T. In the experiment, $\Delta I/I_0$ is around 10^{-2}, making the minimum measurable magnetic field 0.02 T. If higher resolution and higher B_{max} are both required, two all-fiber magnetic field sensors could be co-located. In this scenario, one sensor has a large VL product to obtain the desired resolution; the other one has a small VL product to obtain the desired maximum detected magnetic field by removing the ambiguity of the other sensor.

The Verdet constant of the Tb fiber is dependent on the temperature; for example, $1/V\, dV/dT$ is around 10^{-4}/K for silica.[14] To mitigate the impact of temperature on the measurement results, a fiber-grating temperature sensor could be cascaded or co-located with the magnetic field sensor to monitor the temperature near the magnetic field sensor. In this way, the sensor can give accurate results, providing the device has been calibrated as a function of temperature.

Since the all-fiber magnetic field sensor can measure only magnetic fields parallel to its axis, three orthogonally oriented sensors can be combined to provide a complete three-dimensional magnetic field sensor.

In conclusion, an all-fiber optical magnetic field sensor has been demonstrated. It consists of a fiber Faraday rotator and a fiber polarizer. The fiber Faraday rotator uses a 2-cm-long section of 56-wt%-terbium–doped silicate fiber, and the fiber polarizer is Corning SP1060 single-polarization fiber. The all-fiber optical magnetic field sensor has a sensitivity of 0.49 rad/T and can measure magnetic fields from 0.02 T to 3.2 T.

ACKNOWLEDGMENT

This work was supported by the U.S. Department of Energy Office of Inertial Confinement Fusion under Cooperative Agreement No. DE-FC52-08NA28302, the University of Rochester, and the New York State Energy Research and Development Authority. The support of DOE does not constitute an endorsement by DOE of the views expressed in this article. This work is also supported in part by Wright-Patterson Air Force Research Laboratory under contract FA8650-09-C-5433. The authors would like to acknowledge the technical support of Dr. R. L. Nelson and W. D. Mitchell from AFRL.

REFERENCES

1. J. E. Lenz, Proc. IEEE **78**, 973 (1990).
2. A. Yariv and H. V. Winsor, Opt. Lett. **5**, 87 (1980).
3. H. Okamura, J. Lightwave Technol. **8**, 1558 (1990).
4. V. Radojevic *et al.*, J. Magn. Magn. Mater. **272–276**, e1755 (2004).
5. C.-L. Tien *et al.*, IEEE Trans. Magn. **42**, 3285 (2006).
6. G. W. Day *et al.*, Opt. Lett. **7**, 238 (1982).
7. V. Annovazzi-Lodi, S. Merlo, and A. Leona, J. Lightwave Technol. **13**, 2349 (1995).
8. W. E. Gettys, F. J. Keller, and M. J. Skove, *Physics, Classical and Modern* (McGraw-Hill, New York, 1989).
9. L. Sun, S. Jiang, J. D. Zuegel, and J. R. Marciante, Opt. Lett. **34**, 1699 (2009).
10. L. Sun, S. Jiang, and J. R. Marciante, "All-Fiber Optical Isolator Based on Faraday Rotation in Highly Terbium-Doped Fiber," submitted to Optics Letters.
11. D. A. Nolan *et al.*, Opt. Lett. **29**, 1855 (2004).
12. M. McCaig and A. G. Clegg, *Permanent Magnets in Theory and Practice*, 2nd ed. (Wiley, New York, 1987).
13. J. R. Marciante, N. O. Farmiga, J. P. Kondis, and J. R. Frederick, Opt. Express **11**, 1096 (2003).
14. P. A. Williams *et al.*, Appl. Opt. **30**, 1176 (1991).